Siberian Branch of Russian Academy of Science
BUDKER INSTITUTE OF NUCLEAR PHYSICS



V.N. Baier and V.M. Strakhovenko

# CRYSTAL ASSISTED POSITRON SOURCE EFFICIENCY AT DIFFERENT ENERGIES

Budker INP 98-5

http://www.inp.nsk.su/publications



NOVOSIBIRSK
1998

# Crystal assisted positron source efficiency at different energies

*V.N. Baier and V.M. Strakhovenko*

Budker Institute of Nuclear Physics SB RAS
630090 Novosibirsk, Russia

**Abstract**

Positron yield from crystal and amorphous tungsten is calculated for the kinematics inherent in positron sources. Corresponding electron-photon showers initiated by electrons with energies from a few GeV to several hundreds GeV are considered. Definite advantages of crystal targets especially at high energies are shown.



## 1 Introduction

A positron source is a very important component of the electron-positron collider. Projects of electron-positron linear colliders are under very active development now. For high-energy linear collider the positron source should have intensity much higher than in used now sources. Use of a single crystal in an electromagnetic convertor could increase essentially intensity of produced positrons (into given phase-space). So, single crystals could be used in new kinds of positron sources.

The process of radiation of a photon by the fast charged particle (or pair creation by a photon) when this particle (or the photon) is moving at a small angle $\vartheta_0$ to the direction of its axes or planes differs considerably in comparison with an amorphous medium, as a result of the collective interaction of a certain set of systematically located atoms of the crystal lattice with the incident particle.

A specific property of electromagnetic processes in single crystals is their energy and orientation dependence. For the moderate energy region the angular width of orientation phenomena in the radiation process (channeling radiation) is determined by the Lindhard critical angle $\vartheta_c = \sqrt{2V_0/\varepsilon}$, where $\varepsilon$ is the particle energy and $V_0$ is the scale of the average potential of the axis (plane) relative to which the angle of incidence $\vartheta_0$ is determined.

In the high-energy region (starting from an energy $\varepsilon$ of tens $GeV$) for the angle of incidence $\vartheta_0 \ll V_0/m$ the radiation process depends on electric field on the trajectory only. The pair creation probability in the field of crystal axes falls off exponentially for a photon energy below $\omega_t$, revealing some kind of the threshold behavior. When the initial particle energy $\varepsilon_0(\omega_0) \gg$

$\omega_t$ the coherent mechanisms dominate in both radiation and pair creation processes. Theory of the electromagnetic processes in oriented crystals is given in [1, 2]. It is well known (see [1, 2]) that for some $\varepsilon$ and $\vartheta_0$ effects in crystals are by several times or even by orders of magnitude stronger than in corresponding amorphous media.The most pronounced effects take place at an axial alignment. Therefore, namely this case will be considered in what follows.

The experimental investigation of angular and energy dependence of shower characteristics has been performed in [7]. Our calculations (see [6]) are in a good agreement with results of [7] for $Ge$ crystal.

To estimate the efficiency of a positron source, we should know the number of produced positrons in a definite phase space which can be accepted by the corresponding matching optical system. Typical parameters of such systems mentioned in [4] will be used below, assuming, in particularly, that the energies of accepted positrons are within the following domain: 5 MeV$\leq$ $\varepsilon \leq$25 MeV. Let us remind that at $\vartheta_0 \sim \vartheta_c$ the crystal assisted (coherent) contribution to the pair production probability becomes negligible for photon energies $\omega \leq 10$ GeV. The same is true for photon emission probability at $\varepsilon < 100$ MeV. Therefore, we pay so much attention in Sec.2 to incoherent processes giving the main contribution at low energies. Incoherent contributions to electromagnetic processes are always present in crystals in a slightly modified form as compared to pure amorphous case. They are especially important for a correct description of the pair production process.

In Sec.3 the results obtained by means of the Monte-Carlo simulation procedure are discussed. Calculations have been carried out for an amorphous tungsten and $< 111 >$, $< 001 >$ axes of a tungsten crystal. The initial electron energies up to 300 GeV are considered. The target thickness $L$ was varied in the interval $0 \leq L \leq 2.25$ cm ($\simeq 6.5 L_{rad}$).

## 2 Basic formulae

While moving in a target, the initial and arising charged particles may emit photons and undergo multiple scattering and ionization energy loss. Photons may convert into electron-positron pairs. Many processes, like positron annihilation or photon scattering are ignored in our calculations since their influence on a shower development is small for registered particle energies 5 MeV$\leq \varepsilon(\omega)$ under consideration.

The mechanism of photon emission owing to the regular motion of particles in the field of crystalline axes (coherent contribution) is taken into ac-



count by means of the semi-phenomenological radiation spectrum suggested in [5]. For sufficiently high energies, the spectrum (see eq.(2) in [5]) turns into the intensity spectrum obtained within the constant field approximation (CFA). This approximation was used also to calculate the coherent contribution to the electron-positron pair production probability (eq.(3.5) in [1]). The processes of photon emission and pair production are characterized by their formation times. If an external field does not vary essentially during this time along particle trajectory, the elctromagnetic processes are the same as in a constant ( local ) field and CFA is applicable.

At calculations of the incoherent contribution to the photon emission and pair production probabilities, the inelastic scattering on atomic electrons was disregarded, providing the accuracy of the order of $1/Z$, where $Z$ is the atomic number. Note that an inaccuracy in some probability does not lead directly to the same inaccuracy in shower development description, since many different processes are involved. Starting from the bremsstrahlung cross section obtained in [8] in the Born approximation, and using the Moliére parametrization of the atomic form-factor [9]:

$$\frac{1-F(q)}{q^2} = \sum_{i=1}^{3} \frac{a_i}{q^2 + \lambda^2 m^2 b_i^2}\,,$$
$$a_1 = 0.1,\ a_2 = 0.55,\ a_3 = 0.35\,, \qquad (1)$$
$$b_1 = 6,\ ,\ b_2 = 1.2\,,\ b_3 = 0.3\,,\ \lambda = Z^{1/3}/121\,,$$

we have for the radiation intensity spectrum in an amorphous target:

$$\frac{dI_{br}}{d\omega} = \frac{4Z^2\alpha^3 n}{m^2}\left\{\left[x^2 + \frac{4}{3}(1-x)\right]F_1(s_r) + \frac{1}{9}(1-x) - \right.$$
$$\left. -2s_r\left[\lambda\left(x^2 + 2(1-x)\right) + \frac{2}{3}(1-x)\,F_2(s_r)\right]\right\}. \qquad (2)$$

Here $x = \omega/\varepsilon$, $\alpha = 1/137$ is the fine structure constant, $n$ is the density of atoms,$s_r = mx/[2\varepsilon\lambda(1-x)]$. The functions $F_i$ are

$$F_1(y) = 1 - F_C(\xi^2) + \int_y^{1/\lambda} dt\, t\left[\sum_{i=1}^{3} \frac{a_i\,(t-y)}{b_i^2 + t^2}\right]^2;$$
$$F_2(y) = \int_y^{1/\lambda} dt\left[\sum_{i=1}^{3} \frac{a_i}{b_i^2 + t^2}\right]^2 \left[(t-y)\,(t+2y) - 3yt\ln(t/y)\right], \qquad (3)$$

where $\xi = Z\alpha$. The differential probability of the $e^+e^-$ pair production process in an amorphous target is expressed via the same functions $F_i$, introduced in (3):

$$\frac{dW_p}{dx} = \frac{4Z^2\alpha^3 n}{m^2}\left\{\left[1-\frac{4}{3}x\,(1-x)\right]F_1(s_p) - \frac{1}{9}x\,(1-x) - \right.$$
$$\left. -2s_p\left[\lambda\,(1-2x\,(1-x)) - \frac{2}{3}x\,(1-x)\,F_2(s_p)\right]\right\}, \qquad (4)$$

where now $x = \varepsilon/\omega$, $s_p = m/[2x(1-x)\omega\lambda]$ and $\varepsilon$ is the energy of one of the created particles.

The Coulomb correction to the bremsstrahlung (2) and pair production (4) is represented by the term , $F_C(\xi^2)$ in $F_1$ (3). One usually set $F_C(\xi^2) = f(\xi^2)$, where

$$f(\xi^2) = \xi^2\sum_{k=1}^{\infty}\frac{1}{k(k^2+\xi^2)}\,. \qquad (5)$$

The Coulomb correction to the total probability of the incoherent $e^+e^-$ pair production for photon energies $\omega \geq 5$ MeV has been derived in [10] by fitting the exact low-energy (1.75 MeV$\leq \omega \leq$ 5 MeV) results obtained in [11]. For intermediate energies $\omega \leq 100\ MeV$, the total probability is larger than that obtained with the standard form of the Coulomb correction (5). For $Z = 82$ and $\omega = 5$ MeV it is twice larger as can be seen in Fig.1 of [10]. Basing on the results of [10], we have included the corresponding Coulomb correction directly into spectral distributions (2) and (4) by using the following form of the function $F_C(\xi^2)$

$$F_C(\xi^2) = f(\xi^2)g_1(\beta) - \frac{9\xi^2}{56\beta}\,g_2(\beta,Z)\,. \qquad (6)$$

Here $\beta = \omega/2m$($\varepsilon/2m$ for bremsstrahlung), $f(\xi^2)$ is given by (5), and functions $g_i$ are determined by eqs.(6),(7) of [10]:

$$g_1(\beta) = 1-\frac{9}{7\beta}+\frac{3}{7\beta^2}-\frac{1}{7\beta^3},\ g_2(\beta,Z) = c_1\ln^2\beta + c_2\ln\beta + c_3\,(1-1/\beta)$$
$$+\frac{(1-\xi^2/0.324)}{\beta}\left[5.469\ln^3\beta - 6.3525\ln^2\beta + 4.5465\,(1-1/\beta)\right],$$
$$c_1 = -6.366 + 4.14\xi^2,\quad c_2 = 54.039 - 43.126\xi^2 + 11.264\xi^4,$$
$$c_3 = -52.423 + 49.615\xi^2 - 14.082\xi^4. \qquad (7)$$



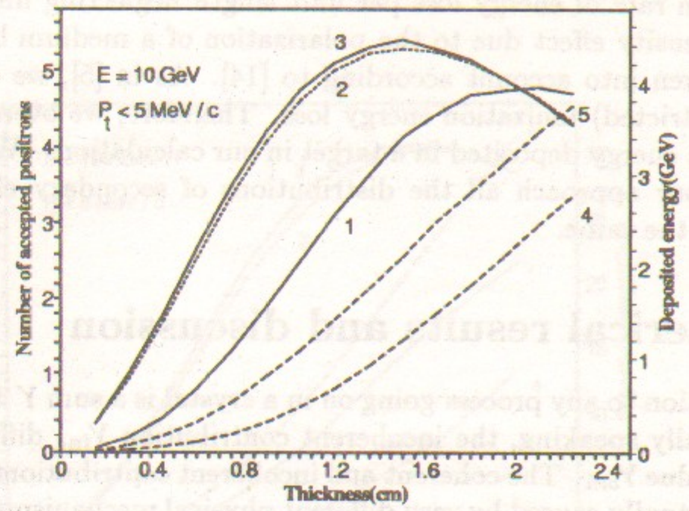


Figure 1: The number of accepted positrons in an amorphous tungsten (curve 1) and in a tungsten crystal (curve 2 for the $< 001 >$-axis, curve 3 for the $< 111 >$-axis) versus target thickness.The deposited energy in an amorphous tungsten (curve 4) and near the $< 111 >$-axis of a tungsten crystal (curve 5). The initial electron energy is $\varepsilon_0 = 10$ GeV.

Using this form of the Coulomb correction $F_C(\xi^2)$ by obtaining the pair production total probability (when integrating over $x$ in (4)), we reproduce within a good accuracy its energy dependence given in [12]. So, our inclusion of the Coulomb correction directly into a spectral distribution is self-consistent.

In crystals, the probabilities of incoherent processes acquire at given momentum transfer $q$ the factor (see [13]) $R(q) = 1-\exp(-q^2u_1^2)$, where $u_1$ is the one-dimensional thermal vibration amplitude of a lattice. Correspondingly, the incoherent processes in crystals will be described by the same formulae (see (2), (4) ) as in amorphous media with the only change:the integrands in (3) should be multiplied by the factor $(1-\exp(-\Gamma^2t^2))$ where $\Gamma = mu_1\lambda$. We have for tungsten $\lambda^{-1} \simeq 28.82$ and $\Gamma^2 \simeq 1/5$ .

The multiple scattering is taken into account within the simplified Bete-Moliére approach neglecting crystalline effects (see corresponding estimate in [5]).

The ionization energy loss by fast electrons and positrons is described in

terms of mean rate of energy loss per unit length neglecting fluctuations as in [5]. The density effect due to the polarization of a medium by a charged particle is taken into account according to [14]. As in [5], we consider the total (not restricted) ionization energy loss. Therefore, we overestimate the quantity of an energy deposited in a target in our calculations. We emphasize that within our approach all the distributions of secondary electrons and positrons are the same.

## 3 Numerical results and discussion

The contribution to any process going on in a crystal is a sum $Y = Y_{coh} + Y_{inc}$ where, generally speaking, the incoherent contribution $Y_{inc}$ differs from the amorphous value $Y_{am}$. The coherent and incoherent contributions to the same process are actually caused by very different physical mechanisms. As a result they are characterized by different spectral distributions and different total probabilities. Therefore, in this paper they were considered as independent processes in Monte-Carlo simulation procedure.

Bearing in mind the assumed properties of a matching optical system, the cut-off value $\varepsilon_f = 5$ MeV was chosen for registered particles and photons. All the results presented below are normalized per one incident electron. At first, we have checked how our modified (but still rather simplified) approach works for an amorphous tungsten target. The results of [15] obtained by the UNIMOD code have been compared with ours for the energy deposited in 0.35cm thick ($L = L_{rad}$) target and for the number of accepted (having transverse momenta $p_\perp \leq 5$ MeV/c and energies 5 MeV$\leq \varepsilon \leq$ 25 MeV) positrons in 1.75cm thick ($L = 5L_{rad}$) target. The initial electron energy was $\varepsilon = 300$ GeV in both cases. Our result for the deposited energy is about 4 percent larger than one obtained in [15] (46.1 MeV instead of 44.3 MeV) what confirms that, as it was expected, we really overestimate the deposited energy but not so much. For the number of accepted positrons the difference is about 14 percent (47.3 instead of 41.4 in [15]). Our numbers is larger mainly due to the used form of the Coulomb correction (6) which significantly increases the total probability as compared with the standard one for photon energies $\omega \leq 50$ MeV. As far as we know, no existent code takes this fact into account.

In Figs. 1, 2, 3 the results of calculations are shown for the number of accepted positrons ($N_{ac}$) and the deposited energy in an amorphous and a crystal tungsten targets. The dependence of the yield on a target thickness is presented for different initial electron energies $\varepsilon_0$ (10 GeV in Fig.1,



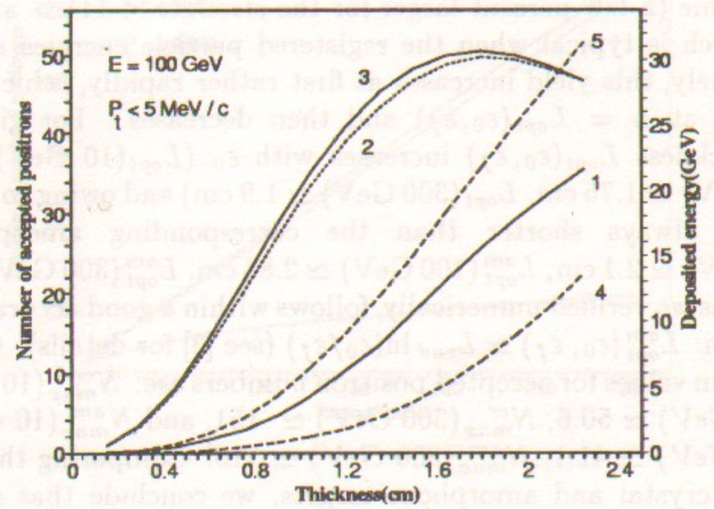


Figure 2: The same as in Fig.1 but for $\varepsilon_0$ =100 GeV.

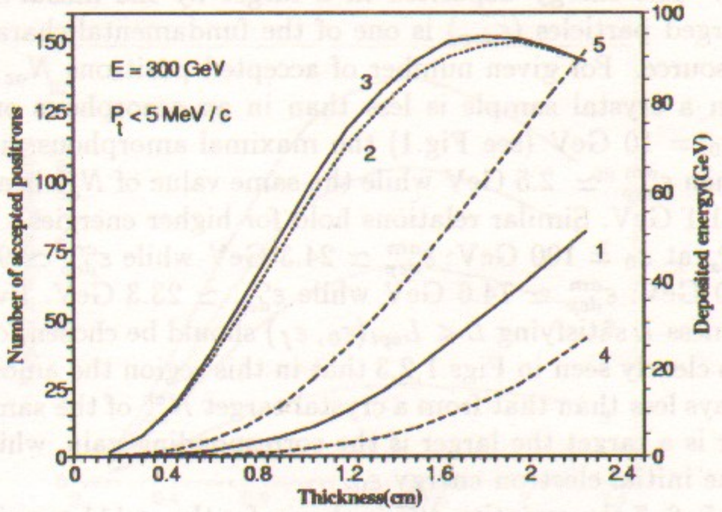


Figure 3: The same as in Fig.1 but for $\varepsilon_0$ =300 GeV.

100 GeV in Fig.2, and 300 GeV in Fig.3). In a crystal case the initial electron momentum is assumed to be aligned along the $< 111 >$ or $< 001 >$ axis. It is seen that the positron yield $N_{ac}$ for two crystal alignments is almost the same (a few percent larger for the stronger $< 111 >$ axis) and has a shape which is typical when the registered particle energies are bounded below. Namely, this yield increases at first rather rapidly, achieves its maximum value at $L = L_{opt}(\varepsilon_0, \varepsilon_f)$ and then decreases. For given $\varepsilon_f$, the optimal thickness $L_{opt}(\varepsilon_0, \varepsilon_f)$ increases with $\varepsilon_0$ ($L_{opt}(10\ \mathrm{GeV}) \simeq 1.5$ cm, $L_{opt}(100\ \mathrm{GeV}) \simeq 1.75$ cm, $L_{opt}(300\ \mathrm{GeV}) \simeq 1.9$ cm) and owing to larger probabilities is always shorter than the corresponding amorphous value ($L^{am}_{opt}(10\ \mathrm{GeV}) \simeq 2.1$ cm, $L^{am}_{opt}(100\ \mathrm{GeV}) \simeq 2.85$ cm, $L^{am}_{opt}(300\ \mathrm{GeV}) \simeq 3.25$ cm). The latter, as we verified numerically, follows within a good accuracy the standard relation: $L^{am}_{opt}(\varepsilon_0, \varepsilon_f) \simeq L_{rad} \ln(\varepsilon_0/\varepsilon_f)$ (see [3] for details). Corresponding maximum values for accepted positron numbers are: $N^{cr}_{max}(10\ GeV) \simeq 5.4$, $N^{cr}_{max}(100\ GeV) \simeq 50.6$, $N^{cr}_{max}(300\ GeV) \simeq 151$, and $N^{am}_{max}(10\ GeV) \simeq 4.8$, $N^{am}_{max}(100\ GeV) \simeq 41.1$, $N^{am}_{max}(300\ GeV) \simeq 116$. Comparing the maximum yields from crystal and amorphous targets, we conclude that such gain is not large, being of 12 to 30 percent depending on the initial electron energy. However, in crystals this yield is obtained at essentially shorter length what, in turn, leads to essentially lower level of deposited energy and target heating. The energy deposited in a target by the initial electron and created charged particles ($\varepsilon_{dep}$) is one of the fundamental characteristics of a positron source. For given number of accepted positrons $N_{ac}$, the energy deposited in a crystal sample is less than in an amorphous one. For example, at $\varepsilon_0 = 10$ GeV (see Fig.1) the maximal amorphous yield $N^{am}_{max}$ is achieved when $\varepsilon^{am}_{dep} \simeq 2.5$ GeV while the same value of $N^{cr}_{ac}$ is accompanied by $\varepsilon^{cr}_{dep} \simeq 1.1$ GeV. Similar relations hold for higher energies. We have for $N^{cr}_{ac} \simeq N^{am}_{max}$ at $\varepsilon_0 = 100$ GeV: $\varepsilon^{am}_{dep} \simeq 24.3$ GeV while $\varepsilon^{cr}_{dep} \simeq 9.1$ GeV and at $\varepsilon_0 = 300$ GeV: $\varepsilon^{am}_{dep} \simeq 74.6$ GeV while $\varepsilon^{cr}_{dep} \simeq 23.3$ GeV. Evidently, the target thickness $L$ satisfying $L < L_{opt}(\varepsilon_0, \varepsilon_f)$ should be chosen for a positron source. It is clearly seen in Figs.1,2,3 that in this region the amorphous yield $N^{am}_{ac}$ is always less than that from a crystal target $N^{cr}_{ac}$ of the same thickness. The thinner is a target the larger is the corresponding gain, which increases also with the initial electron energy $\varepsilon_0$.

In Figs. 5, 6, 7 the quantity $N^{cr}_{ac}$ is shown for the $< 111 >$ axis depending on a crystal thickness $L$, $\varepsilon_0$ and the maximal transverse momentum accepted $p_\perp$. The condition 5 MeV $\leq \varepsilon \leq$ 25 MeV for accepted positrons was not changed. The similarity of curves in Figs. 5, 6, 7 means that the angular distribution of soft positrons is qualitatively the same for different $\varepsilon_0$ with the magnitude roughly proportional to $\varepsilon_0$. It turns out that at given $\varepsilon_0$



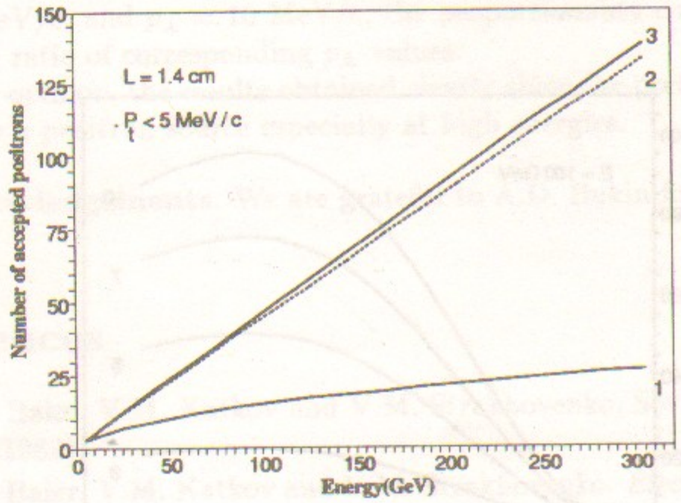


Figure 4: The number of accepted positrons in an amorphous tungsten (curve 1) and in a tungsten crystal (curve 2 for the $< 001 >$-axis, curve 3 for the $< 111 >$-axis) versus initial electron energy. The target thickness is $L = 1.4$ cm, $p_\perp \leq 5$ MeV/c.

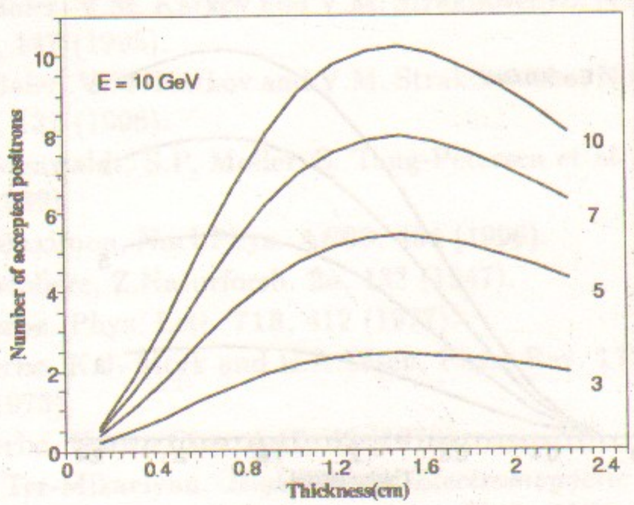


Figure 5: The number of accepted positrons in a tungsten crystal at $< 111 >$-axial alignments versus a crystal thickness for different values of boundary transverse momentum $p_\perp$ indicated (in MeV/c) near corresponding curves. The initial electron energy is $\varepsilon_0 = 10$ GeV.

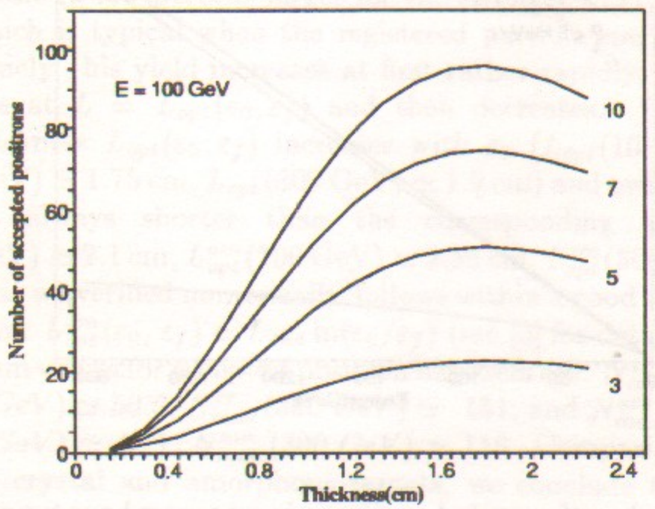


Figure 6: The same as in Fig.4 but for $\varepsilon_0 = 100$ GeV.

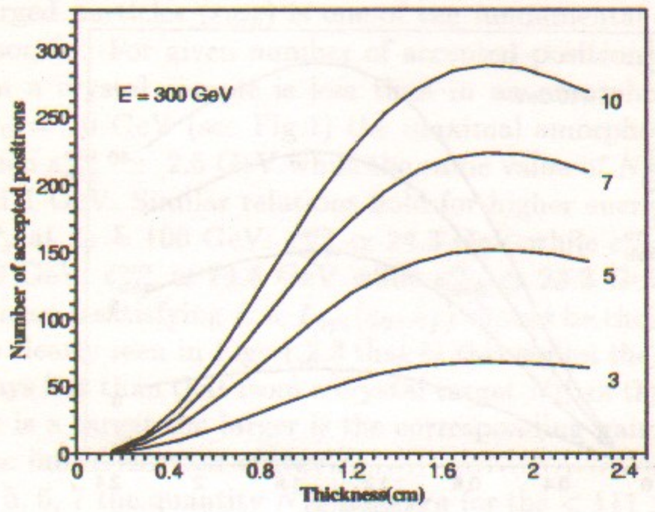


Figure 7: The same as in Fig.4 but for $\varepsilon_0 = 300$ GeV.



the curves calculated for different $p_\perp$ are similar too. For $p_\perp = 5$ MeV/c, $p_\perp = 7$ MeV/c, and $p_\perp = 10$ MeV/c, the proportionality coefficient roughly equals the ratio of corresponding $p_\perp$ values.

To our opinion, the results obtained clearly show the preference of crystal targets for a positron source especially at high energies.

**Acknowledgements**. We are grateful to A.D. Bukin for fruitful discussions.

## References

[1] V.N. Baier, V.M. Katkov and V.M. Strakhovenko, Sov. Phys. USP. **32**, 972 (1989).

[2] V.N. Baier, V.M. Katkov and V.M. Strakhovenko, *Electromagnetic Processes at High Energies in Oriented Single Crystals*, World Scientific Publishing Co, Singapore, 1998.

[3] V.N. Baier, V.M. Katkov and V.M. Strakhovenko, Nucl. Instr. and Meth. **B27**, 360 (1987).

[4] X. Artru, V.N. Baier, R. Chehab, A. Jejcic, Nucl. Instr. and Meth. **A344**, 443 (1994).

[5] V.N. Baier, V.M. Katkov and V.M. Strakhovenko, Nucl. Instr. and Meth. **B103**, 147 (1995).

[6] V.N. Baier, V.M. Katkov and V.M. Strakhovenko, Nucl. Instr. and Meth. **B119**, 131 (1996).

[7] R. Medenwaldt, S.P. Moller, S. Tang-Petersen et al., Phys. Lett. **B227**, 483 (1989).

[8] L.C. Maximon, Nucl.Phys. **A609**, 454 (1996).

[9] G.Z. Moliére, Z.Naturforsh. **2a**, 133 (1947).

[10] I. Øverbø, Phys. Lett. **718**, 412 (1977).

[11] I. Øverbø, K.J. Mork and H.A.Olsen, Phys. Rev. **175**, 1978 (1968); **A8**, 668 (1973).

[12] I. Øverbø, Nuovo Cim. **A47**, 43 (1978).

[13] M.L. Ter-Mikaelyan. *High-Energy Electromagnetic Processes in Condensed Media*, Wiley-Interscience, New York, 1972.

[14] R.M. Sternheimer, S.M. Seltzer, and M.J. Berger, Atomic Data and Nucl. Data Tables, **30**, 261 (1984).

[15] A.D. Bukin, private communication, 1997.

*V.N. Baier and V.M. Strakhovenko*

**Crystal assisted positron source efficiency at different energies**

*В.Н. Байер, В.М. Страховенко*

**Эффективность позитронного источника с использованием кристаллов при разных энергиях**

Budker INP 98-5

Ответственный за выпуск А.М. Кудрявцев
Работа поступила 4.02. 1998 г.

Сдано в набор 27.04.1998 г.
Подписано в печать 4.02.1998 г.
Формат бумаги 60×90 1/16 Объем 1.1 печ.л., 0.9 уч.-изд.л.
Тираж 100 экз. Бесплатно. Заказ N° 5

Обработано на IBM PC и отпечатано на
ротапринте ИЯФ им. Г.И. Будкера СО РАН,
*Новосибирск, 630090, пр. академика Лаврентьева, 11.*